Electronic Effects in Transition Metal Porphyrins. 8. The Effect of Porphyrin Substituents, Axial Ligands, "Steric Crowding", Solvent, and Temperature on the ^{57}Fe Chemical Shifts of a Series of Model Heme Complexes

Larry M. Mink,*[1] Jayapal Reddy Polam,* Kenner A. Christensen, Michael A. Bruck, and F. Ann Walker*

Contribution from the Department of Chemistry, University of Arizona, Tucson, Arizona 85721

Received March 24, 1995[⊗]

Abstract: The ^{57}Fe chemical shifts of a series of 94.5% ^{57}Fe enriched model heme complexes (those of tetraphenylporphyrin, TPP, and two of its *p*-phenyl substituted derivatives, tetramesitylporphyrin, TMP, and octaethylporphyrin, OEP), for which trimethylphosphine serves as at least one of the axial ligands, have been measured by recording the ^{31}P NMR spectrum using double resonance at the appropriate ^{57}Fe frequency. The discovery of an approximate correlation between ^{31}P and ^{57}Fe chemical shifts makes it easy to predict the ^{57}Fe chemical shift of new complexes, thus simplifying the search for the proper decoupling frequency. The ^{57}Fe chemical shifts of substituted phenyl TPP complexes increase as the electron-donating nature of the substituents increases, and most OEP complexes have chemical shifts that are 200–250 ppm larger than their TPP counterparts; both of these trends are attributed to increased π donor characteristics that increase the magnitude of the paramagnetic screening constant, σ^{para}. Mixed axial ligand complexes where trimethylphosphine is one of the ligands have larger ^{57}Fe chemical shifts when the other ligand (L) is a strong σ donor/weak π acceptor, but within a group of closely related ligands such as 4-substituted pyridines, the weakest σ donor/strongest π acceptor ligand produces the largest ^{57}Fe chemical shift (4-CNPy > Py > 4-NMe$_2$Py), in line with the predictions of the Ramsey formula for σ^{para}. Solvent effects on the ^{57}Fe chemical shift of [TMPFe(PMe$_3$)$_2$] are small and, in distinction to 6-coordinate low-spin cobalt(III) porphyrinates, do not follow any common measures of solvent polarity or donor strength (dielectric constant, Gutmann's donor number, Reichardt's E_T). ^{31}P and ^{57}Fe chemical shifts both show linear temperature dependence, but with opposite slopes. The structures of two (PMe$_3$)$_2$ complexes of iron(II) porphyrinates, [(*p*-OCH$_3$)$_4$TPPFe(PMe$_3$)$_2$]·2C$_6$D$_6$ and [OEPFe(PMe$_3$)$_2$], have also been determined. In both cases the porphyrinate core is essentially planar and the axial trimethylphosphine ligands have their methyl groups in staggered conformation.

Introduction

Hemes and heme proteins have diverse roles in biological systems that continue to unfold, even after many years of investigation by a large number of scientists from many specialized disciplines.[2] All of the heme proteins have in common an active site which is an iron porphyrinate complex. Determination of the 3-dimensional structures of heme proteins and the elucidation of the detailed structure of the heme center, as well as the correlation of structural features to the function of the protein, relies increasingly on high-resolution NMR spectroscopic methods. Both diamagnetic Fe(II) and paramagnetic Fe(III) hemes and heme proteins have been investigated in detail by ^{1}H NMR spectroscopy.[3] However, while the paramagnetism of Fe(III) porphyrinates and ferriheme proteins makes the proton NMR spectra of these species exquisitely sensitive to subtle perturbations of electron density caused by changes in substituents, axial ligands, axial ligand plane orientation, or protein pocket residues, the same is not true of low-spin, diamagnetic Fe(II) porphyrins and heme proteins. Since electron transfer between ferri- and ferrocytochromes *a*, *b*, *c*, *d*, *f*, and *o usually* involves low-spin Fe(III) and low-spin Fe(II), sensitive probes of the factors that affect the orbital energies and electron distribution within the diamagnetic Fe(II) center are needed. Both ^{1}H and ^{13}C NMR spectroscopy of diamagnetic hemes are relatively insensitive to such factors as porphyrin planarity and axial ligand σ- and π-bonding interactions, and they do not provide direct information as to the effects of porphyrin substituents on the electron density or electron distribution at the Fe(II) center. (For example, the ^{13}C chemical shifts for ^{13}C-labeled carbonyl groups in model hemes and heme proteins cover a total chemical shift range of only about 10 ppm;[4,5] ^{1}H chemical shifts of porphyrin or axial ligand substituents show much smaller chemical shift ranges.) Other spectroscopic techniques such as resonance Raman, infrared, and UV–visible spectroscopy also do not provide direct information concerning the effect of porphyrin substituents, axial ligand interactions, and electronic asymmetry at the Fe(II) center. Mössbauer spectroscopy is potentially a useful tool for *directly* probing the electron density distribution at the iron center. However, the range of isomer shifts ($0.14 \leq \delta \leq 0.51$ mm/s)

[⊗] Abstract published in *Advance ACS Abstracts*, August 15, 1995.

(1) Present Address: Department of Chemistry, California State University, 5500 University Parkway, San Bernardino, CA 92407.

(2) Walker, F. A.; Simonis, U. Iron-Porphyrin Chemistry. In *Encyclopedia of Inorganic Chemistry*; King, R. B., Ed.; Wiley & Sons Ltd.: London, 1994; Vol. 4, pp 1785–1846.

(3) Walker, F. A.; Simonis, U. Proton NMR Spectroscopy of Model Hemes. In *Biological Magnetic Resonance, Vol. 12: NMR of Paramagnetic Molecules*; Berliner, L. J., Reuben, J., Eds.; Plenum Press: New York 1993; pp 133–274.

(4) (a) Moon, R. B.; Richards, J. H. *Biochemistry* **1974**, *13*, 3437. (b) Battersby, A. R.; Bartholomew, A. J.; Nitta, T. *J. Chem. Soc., Chem. Commun.* **1983**, 1291. (c) Boitrel, B.; Lecas-Nawrocka, A.; Rose, E. *Tetrahedron Lett.* **1991**, *32*, 2129.

(5) (a) La Mar, G. N.; Viscio, D. B.; Budd, D. L.; Gersonde, K. *Biochem. Biophys. Res. Commun.* **1978**, *82*, 19. (b) La Mar, G. N.; Dellinger, C. M.; Sankar, S. S. *Biochem. Biophys. Res. Commun.* **1985**, *128*, 628.

0002-7863/95/1517-9329$09.00/0

and quadrupole splittings ($0.35 \leq \Delta E_Q \leq 1.52$ mm/s)[6,7] reported thus far for diamagnetic iron(II) porphyrinates is relatively small, and the parameters are insensitive to the nature of the porphyrin substituents.[7]

In contrast to the above-listed techniques, the NMR chemical shift range of the ^{57}Fe nucleus is at least 12 000 ppm,[8-10] and hence ^{57}Fe NMR is potentially an extremely powerful and direct probe of the asymmetry of the electron distribution and other covalency effects at the iron nucleus of diamagnetic Fe(II) porphyrinates. However, ^{57}Fe ($I = {}^1/_2$) is of low natural abundance (2.19%) and has an extremely low magnetogyric ratio ($\nu_{Fe} = 16.2$ MHz at 11.75 T, for which $\nu_H = 500.1$ MHz), leading to a small Boltzmann population difference between the two spin states. The combination of low natural abundance and low magnetogyric ratio make the naturally abundant ^{57}Fe nucleus only 7.4×10^{-7} as sensitive as the proton in natural abundance. In addition, some ^{57}Fe resonances have extremely long T_1 relaxation times,[11] although this does not appear to be a serious problem with Fe(II) porphyrinates.[9,12,13] Isotopic enrichment helps the sensitivity problem, but even so, direct detection of ^{57}Fe signals of model hemes or heme proteins requires hours to days of NMR time, and large volumes of enriched sample. For this reason, several research groups, including ours, have developed indirect detection methods for ^{57}Fe based on higher γ nuclei such as ^{15}N,[14,15] ^{13}C[5,10d,16] and ^{31}P[10a-c,17] that allow ^{57}Fe chemical shifts to be determined more easily. Our method, to be described in more detail in the Experimental Section, relies upon trimethylphosphine, PMe_3, being one or both of the axial ligands of the Fe(II) porphyrinates and utilizes the sensitive ^{31}P nucleus as the detected signal. The scalar coupling of ^{57}Fe to the ^{31}P nucleus of PMe_3, which results in the observed ^{31}P doublet, is then decoupled when the proper ^{57}Fe decoupling frequency is used. This method allows the measurement of ^{57}Fe chemical shifts of new complexes in 5 mm NMR tubes in as little as 20 min.[17] In the work reported herein, we have utilized this technique to investigate a series of model hemes in which the porphyrinate ligand is a tetraphenylporphyrinate (TPP) derivative or tetramesityl- (TMP) or octaethylporphyrinate (OEP).

There have now been a number of reports of ^{57}Fe chemical shifts of model hemes[5,9,14,17-21] and several heme proteins.[5,9,12,13,21,22] Unfortunately, different conditions (solvent, temperature, porphyrin substituents, axial ligands) have been used to obtain these chemical shifts, which makes it difficult to interrelate the available data to delineate the factors that affect the ^{57}Fe chemical shifts of these complexes. Of the data currently available, the ^{57}Fe chemical shift of the (His-Met)-ligated heme protein cytochrome *c* (11 197 ppm),[9] is unique compared to those of other heme axial ligand combinations reported thus far (bis(phosphine), 7627-7664 ppm;[17] bis(pyridine) or bis(pyrrolidine), 7341, 7258 ppm;[14] CO-aromatic amine, 8041-8234 ppm,[5,12,18,19,21] except for cases of steric hindrance to linear CO binding;[19] imidazole-isocyanide, 9223-9257 ppm[13]). A possible reason for this very different ^{57}Fe chemical shift for ferrocytochrome *c* has been suggested by Baltzer[9] and Oldfield,[13] who believe that the most important factor in determining the chemical shifts and line widths in these systems is the anisotropy of the chemical shift tensor, $|\delta_\perp - \delta_{||}|$, where $\delta_\perp$ is determined by the porphyrin ring and is fairly similar for all Fe(II) porphyrinates, while $\delta_{||}$ is determined by the axial ligands and varies significantly with axial ligand combination. In this regard, it is interesting to note that most ^{57}Fe chemical shifts reported thus far are for complexes having one relatively weak σ-donor, strong π acceptor (CO, RNC, or PMe_3) and one relatively strong σ donor (pyridine, imidazole, $RSCH_3$, or RNH_2). The exceptions to this ligand combination in the systems listed above are the cases of two π acceptors presented in this work, cytochrome *c* and the bis(pyridine) and bis(pyrrolidine) complexes of TPPFe(II). Further comment on these systems will be provided in the Discussion section.

In contrast to the suggestion of Baltzer and Oldfield, Sams[6] and Sato[7] earlier each concluded, from Mössbauer spectroscopic data, that the porphyrinate macrocycle has an "electron sink capability", which *compensates for the electronic properties of axial ligands*. The conclusions obtained from NMR[9,13] and Mössbauer[6,7] spectroscopies are thus in contradiction, and suggest the need for further investigations. Part of the goal of our study has been to systematically probe the effect of porphyrin substituents and axial ligands on the ^{57}Fe chemical shift.

We previously observed a rough correlation between the ^{57}Fe and ^{31}P chemical shifts of a series of [(RTPP)^{57}Fe(PMe_3)(L)] complexes (RTPP = a symmetrically R-substituted tetraphenylporphyrinate, L = PMe_3, CO, isocyanide, aliphatic amine, imidazole, pyridine, or thioether).[17] We have now further extended our studies of model iron porphyrinates to include the tetramesitylporphyrinate (TMP) and octaethylporphyrinate (OEP) series of complexes in order to delineate the effects of heme substituents on the ^{57}Fe chemical shift and have found that the approximate correlation observed previously is better described as two clusters of ^{57}Fe-^{31}P shifts. We have also investigated the temperature and solvent dependences of the ^{57}Fe and ^{31}P chemical shifts of several of these complexes.

Experimental Section

Materials, Methods, and Preparations. Reagent grade chemicals and solvents were purchased from Aldrich and Matheson and deuterated solvents from Cambridge Isotopes. Iron-57 metal (94.5% enriched) was purchased from New England Nuclear, Isotec, or Cambridge Isotopes, and octaethylporphyrin and tetramesitylporphyrin were purchased from Midcentury. Chromatographic grade silica gel was purchased form Davison Chemical.

Syntheses of complexes were performed under argon using standard Schlenk and inert-atmosphere techniques. All solvents were of special

(6) Sams, J. R.; Tsin, T. B. In *The Porphyrins*; Dolphin, D., Ed.; Academic Press: New York, 1978; Vol. IV, pp 425-478.
(7) Ohya, T.; Morohoshi, H.; Sato, M. *Inorg. Chem.* **1985**, *23*, 1303.
(8) (a) von Philipsborn, W. *Pure Appl. Chem.* **1986**, *58*, 513. (b) Jenny, T.; von Philipsborn, W.; Kronenbitter, J.; Schwenk, A. J. *Organomet. Chem.* **1981**, *205*, 211. (c) Webb, G. A. *Annu. Rep. NMR Spectrosc.* **1991**, 23.
(9) Baltzer, L. *J. Am. Chem. Soc.* **1987**, *109*, 3479.
(10) (a) Benn, R.; Brevard, C. *J. Am. Chem. Soc.* **1986**, *108*, 5622. (b) Benn, R.; Brenneke, H.; Frings, A.; Lehmkuhl, H.; Mehler, G.; Rufinska, A.; Wildt, T. *J. Am. Chem. Soc.* **1988**, *110*, 5661. (c) Benn, R.; Rufinska, A. *Magn. Reson. Chem.* **1988**, *26*, 895. (d) Benn, R.; Rufinska, A.; Kralik, M. S.; Ernst, R. D. *J. Organomet. Chem.* **1989**, *375*, 115.
(11) Schwenck, A. *J. Magn. Reson.* **1971**, *5*, 376.
(12) Baltzer, L.; Becker, E. D.; Averill, B. A.; Hutchinson, J. M.; Gansow, O. *J. Am. Chem. Soc.* **1984**, *106*, 2444.
(13) Chung, J.; Lee, H. C.; Oldfield, E. *J. Magn. Reson.* **1990**, *90*, 148.
(14) Nozawa, T.; Sato, M.; Hatano, M.; Kobayashi, N.; Osa, T. *Chem. Lett.* **1983**, 1289.
(15) Morishima, I.; Inabushi, T.; Sato, M. *J. Chem. Soc., Chem. Commun.* **1978**, 106.
(16) Koridze, A. A.; Astakhova, N. M.; Petrovskii, P. V. *J. Organomet. Chem.* **1983**, *254*, 345.
(17) Mink, L. M.; Christensen, K. A.; Walker, F. A. *J. Am. Chem. Soc.* **1992**, *114*, 6930.
(18) Baltzer, L.; Landergren, M. *J. Chem. Soc., Chem. Commun.* **1987**, 32.
(19) Baltzer, L.; Landergren, M. *J. Am. Chem. Soc.* **1990**, *112*, 2804.
(20) (a) Morishima, I.; Inubushi, T. *J. Chem. Soc., Chem. Commun.* **1978**, 3, 106. (b) Morishima, I.; Hayashi, T.; Insushi, T.; Yonezawa, T. *J. Chem. Soc., Chem. Commun.* **1979**, 483.
(21) Lee, H. C.; Gard, J. K.; Brown, T. L.; Oldfield, E. *J. Am. Chem. Soc.* **1985**, *107*, 4087.
(22) Baltzer, L.; Becker, E. D.; Tschudin, R. G.; Gansow, O. A. *J. Chem. Soc, Chem. Commun.* **1985**, 1040.

grade quality and were dried, distilled, and degassed before use. All NMR solvents were dried and degassed by repeated freeze–pump–thaw before use, and spectra were obtained in C_6D_6, d_8-toluene, $CDCl_3$, dichloromethane, and tetrahydrofuran. ^{31}P NMR spectra were recorded on a Brucker AM 500 spectrometer equipped with a 5 mm $\{^{57}Fe,^1H\}^{31}P$ probe built by Cryomagnetic Systems (Indianapolis, IN). Four separate frequencies are entered into the probe: the deuterium lock frequency (76.0 MHz), proton decoupling frequency (500.1 MHz), ^{57}Fe decoupling frequency (~16.2 MHz), and the ^{31}P observe frequency (202.5 MHz). The ^{57}Fe decoupling frequency was generated by a PTS 160 frequency synthesizer locked to the 10 MHz reference frequency of the spectrometer. The frequency was checked with a Hewlett-Packard 5383A frequency counter, also locked to the 10 MHz spectrometer reference frequency. The ^{57}Fe decoupling frequency was amplified by an ENI 310 L amplifier and passed through a 16 MHz band pass filter. A 200 MHz band pass filter was placed between the probe and the ^{31}P preamplifier. All ^{31}P spectra were externally referenced to 85% H_3PO_4. ^{57}Fe chemical shifts were externally referenced to neat $Fe(CO)_5$.

^{57}Fe Chemical Shift Detection. By stepping through the iron frequency range near 16.2 MHz in 100 Hz (~6.3 ppm) increments using an iron decoupling power of 0.5 W, the collapse of the $^{57}Fe-^{31}P$ doublet (J_{Fe-P} = 40–59 Hz) was detected when the ^{57}Fe resonant frequency was reached. Upon detection of the collapsed ^{31}P doublet the iron decoupling power was decreased to 0.1 W, and a more precise measurement of the resonant iron frequency was made by stepping through in 10 Hz (~0.6 ppm) increments.

Synthesis of [Por$^{57}Fe^{III}Cl$], Where Por = TPP, (p-Cl)$_4$TPP, (p-OCH$_3$)$_4$TPP, and TMP, OEP. Iron-57 was inserted into the corresponding porphyrin free bases forming [Por$^{57}Fe^{III}Cl$] as described previously.[23] In the case of iron insertion into TMP and OEP, iron-57 metal chips were used instead of iron powder. Two batches of ^{57}Fe metal chips (39.2 mg, 0.66 mmol) were dissolved in 60 mL of glacial acetic acid by refluxing for 2 days under nitrogen with periodic bubbling of HCl(g) through the solution. A 2-fold excess of TMP (1.0345 g, 1.32 mmol) and OEP (0.705 g, 1.32 mmol) was dissolved in 70 mL of 1:1 glacial acid/pyridine, one in each reaction solution. The iron solution was added to the degassed solution containing TMP or OEP and refluxed overnight under nitrogen. The isolation of [TMP$^{57}Fe^{III}$-Cl] and [OEP$^{57}Fe^{III}Cl$] from the reaction mixture was performed in the same fashion as [TPP$^{57}Fe^{III}Cl$].[23] The iron-57 insertion into TMP and OEP proceeded in 98% yield based on ^{57}Fe as the limiting reagent, and 89% of the excess TMP and OEP was recovered.

Synthesis of [Por$^{57}Fe^{II}$(PMe$_3$)$_2$], Where Por = TPP, (p-Cl)$_4$TPP, (p-OCH$_3$)$_4$TPP, TMP, and OEP. Two methods were utilized for the reduction of [Por$^{57}Fe^{III}Cl$]. In the first, [Por$^{57}Fe^{III}Cl$] (0.021 g, ~0.025 mmol) (Por = TPP, (p-Cl)$_4$TPP and (p-OCH$_3$)$_4$TPP) was reduced in the glovebox to [Por$^{57}Fe^{II}$] with zinc amalgam[24] (1.28 g, 4.8 mmol) in degassed C_6D_6 (1 mL). After about 2 h of stirring over zinc amalgam, [Por$^{57}Fe^{II}$] in C_6D_6 was syringed directly into a gas tight 5 mm NMR tube fitted with a septum cap and removed from the glovebox. [Por^{57}-Fe^{II}(PMe$_3$)$_2$] was formed by NMR titration of a degassed solution of 1.0 M PMe$_3$ in toluene (Aldrich, ~30 μL) into the NMR tube containing [Por$^{57}Fe^{II}$] using gas tight syringes. Upon addition of PMe$_3$ to [Por^{57}-Fe^{II}] the color of the solution turns from a dark red to greenish brown.

The above method was found to produce incomplete reduction of [OEP$^{57}Fe^{III}Cl$] and [TMP$^{57}Fe^{III}Cl$], and hence a second method of reduction was developed. [OEP$^{57}Fe^{III}Cl$] (0.010 g, 0.016 mmol) or [TMP$^{57}Fe^{III}Cl$] (0.010 g, 0.0115 mmol) was placed in Schlenk flasks and a large excess of $NaBH_4$ (0.030 g, 0.78 mmol) in dry THF (10 mL) was added. The reaction was stirred for 18 h in order to completely reduce Fe(III) to Fe(II). Then 30 μL (a slight excess) of 1.0 M PMe$_3$ in toluene (Aldrich) was added to the Schlenk flask. The reaction appeared to be instantaneous, but the solution was stirred for 15 min. The color of the (PMe$_3$)$_2$Fe^{II}TMP and -OEP complexes is greenish brown and red, respectively. The solvent was taken off under reduced pressure and the product dried for 4 h under vacuum. The Schlenk flasks were transferred into the glovebox and the products were dissolved in the chosen NMR solvent (1 mL). Each solution was filtered into an NMR tube through a Pasteur pipet filled with glass wool.

X-ray quality single crystals of [(p-OCH$_3$)$_4$TPP$^{57}Fe^{II}$(PMe$_3$)$_2$] and [OEP$^{57}Fe^{II}$(PMe$_3$)$_2$] were formed by slow evaporation of the solvent C_6D_6 and d_8-toluene, respectively, after 3 weeks in the glovebox.

Synthesis of [Por$^{57}Fe^{II}$(PMe$_3$)(L)], Where L = CO, n-Butylisocyanide, n-Butylamine, N-Methylimidazole, 2-Methylimidazole, Benzyl Methyl Sulfide, 4-(Dimethylamino)pyridine, Pyridine, and 4-Cyanopyridine. Ligand L was titrated into the NMR tube containing [TPP$^{57}Fe^{II}$] (0.021 g, ~0.025 mmol) to form [TPP$^{57}Fe^{II}$(L)$_2$]. Compound [TPP$^{57}Fe^{II}$(L)$_2$] was then titrated with a 1.0 M solution of PMe$_3$ in toluene (~26 μL) to form the mixed axial ligand complex [TPP^{57}-Fe^{II}(PMe$_3$)(L)].[25] In the case of CO, addition was performed by slow bubbling of the gas through Teflon-tipped needles. All ligands L that were liquids were degassed by the freeze–pump–thaw method before addition. All additions of liquids were performed through gas-tight syringes. In the case of mixed ligand complexes of OEP$^{57}Fe^{II}$ and TMP$^{57}Fe^{II}$, known quantaties of each starting material, [OEP$^{57}Fe^{III}$Cl] (0.010 g, 0.016 mmol) or [TMP$^{57}Fe^{III}$Cl] (0.010 g, 0.0115 mmol), and $NaBH_4$ (0.030 g, 0.78 mmol) were placed in Schlenk flasks followed by 10 mL of dry degassed THF and the mixture was stirred for 18 h. The solution was then titrated with a slight excess over stoichiometric amount of Lewis base and a stoichiometric amount (16 μL for OEP, 11 μL for TMP) of PMe$_3$ (1.0 M in toluene) to form the mixed ligand complex. In the formation of the CO mixed ligand complexes, CO gas was bubbled through the reaction mixture of the reduced Fe^{II} porphyrinate which was then titrated with a stoichiometric amount of PMe$_3$ (1.0 M in toluene) and stirred for 15 min. The solvent was taken off under reduced pressure, NMR solvent (1 mL) was added, and the solution was filtered into an NMR tube in the glovebox. All [Por$^{57}Fe^{II}$(PMe$_3$)$_2$] and [Por$^{57}Fe^{II}$(PMe$_3$)(L)] samples are stable under inert atmosphere at room temperature over the course of weeks.

X-ray Crystallography. The structures of the complexes [(OEP)-Fe^{II}(PMe$_3$)$_2$] and [(p-OCH$_3$)$_4$TPP)-Fe^{II}(PMe$_3$)$_2$]·2C$_6$D$_6$ have been determined by X-ray crystallography. A summary of crystallographic data and results is given in Table 1. Bond lengths and bond angles are given in Tables S1-S4, supporting information.

Results and Discussion

A. Preparation of Compounds. The complexes studied were isotopically enriched to 94.5% with ^{57}Fe. The formation of [TPP$^{57}Fe^{II}$(PMe$_3$)$_2$] upon addition of PMe$_3$ was monitored by ^1H NMR. All resonances associated with paramagnetic 4-coordinate [TPP$^{57}Fe^{II}$] (phenyl o-H, 21.3 ppm; p-H 12.7, ppm; m-H, 12.5 ppm; pyrrole-H, 4.0 ppm)[28] are shifted into the diamagnetic region upon the formation of [TPP$^{57}Fe^{II}$(PMe$_3$)$_2$] (phenyl o-H, 8.07 ppm; p, m-H, 7.42 ppm; pyrrole-H, 8.68 ppm);[25] the proton resonance for the coordinated PMe$_3$ methyl protons was observed at −2.62 ppm, while uncoordinated PMe$_3$, when in excess, was observed at 1.02 ppm. The detection of coordinated PMe$_3$ in the presence of uncoordinated PMe$_3$ indicates that the exchange rate is slow on the ^1H NMR time scale. This slow exchange rate had previously been reported.[29] The resonance for coordinated PMe$_3$ is shifted to higher shielding due to the ring current shielding of the porphyrinato ring. Formation of diamagnetic TMP– and OEP–iron com-

(23) Walker, F. A.; Huynh, B. H.; Scheidt, W. R.; Osvath, S. R. *J. Am. Chem. Soc.* **1986**, *108*, 5288.

(24) Landrum, J. T.; Hatano, K.; Scheidt, W. R.; Reed, C. A. *J. Am. Chem. Soc.* **1980**, *102*, 6729.

(25) Sodano, P.; Simonneaux, G. *J. Chem. Soc., Dalton Trans.* **1988**, 2615.

(26) Frenz, B. A. The Enraf-Nonius CAD 4 SDP–A Real-time System for Concurent X-Ray Data Collection and Crystal Structure Determination. In *Computing in Crystallography*; Schenk, H., Olthof-Hazelkamp, R., vanKonigsveld, H., Bassi, G. C., Eds.; Delft University Press: Delft, 1978; pp 64–71.

(27) *MolEN: An Interactive Structure Solution Procedure*; Enraf-Nonius: Delft, 1990.

(28) Goff, H.; La Mar, G. N.; Reed, C. A. *J. Am. Chem. Soc.* **1977**, *99*, 3641.

(29) (a) Bondon, A.; Petrinko, P.; Sodano, P.; Simmonneaux, G. *Biochim. Biophys. Acta* **1986**, *872*, 163. (b) Bondon, A.; Sodano, P.; Crescau, C. T. *Biochim. Biophys. Acta* **1987**, *914*, 289.

Table 1. Summary of Crystal Data and Intensity Collection Information for Bis(trimethylphosphine)[5,10,15,20-tetra(*p*-methoxyphenyl)porphyrinato]iron(II), [(*p*-OCH_3)TPP$^{57}Fe^{II}(PMe_3)_2$], and Bis(trimethylphosphine)(octaethylporphyrinato)iron(II), [OEP$^{57}Fe^{II}(PMe_3)_2$]

	[(*p*-OCH_3)$_4$TPP$Fe^{II}(PMe_3)_2$]	[OEP$Fe^{II}(PMe_3)_2$]
	A. Crystal Data	
formula	$FeP_2O_4N_4C_{54}H_{54}\cdot 2C_6H_6$	$Fe_1P_2N_4C_{42}H_{62}$
FW	1097.08	740.78
F(000)	578	796
crystal dimensions, mm	0.20 × 0.17 × 0.42	0.15 × 0.28 × 0.33
peak width at half-height, deg	0.99	0.20
Mo Kα radiation (λ, Å)	0.70930	0.71073
temp, °C	23 ± 1	21 ± 1
crystal class	triclinic	monoclinic
space group	$P\bar{1}$	$P2_1/c$
cell parameters		
a, Å	10.794(1)	9.948(1)
b, Å	11.716(1)	20.643(2)
c, Å	12.860(1)	10.130(1)
α, deg	73.52(20)	
β, deg	65.94(26)	98.03(65)
γ, deg	82.44(26)	
V, Å^3	1423.7	2059.9(5)
Z	1	2
ϱ, g/cm^3	1.28	1.19
μ, cm^{-1}	3.7	4.7
	B. Intensity Measurements	
instrument	Enraf-Nonius CAD4	Enraf-Nonius CAD4
monochromator	graphite crystal, incident beam	graphite crystal, incident beam
attenuater	Zr Foil, factor 13.6	Zr Foil, factor 13.6
scan type	$\omega-2\theta$	$\omega-2\theta$
scan rate, deg/min	1−7	2−7 (in omega)
scan width, deg	$\theta = 0.6 + 0.340\tan\theta$	$\theta = 0.8 + 0.340\tan\theta$
maximum 2θ, deg	50.0	50.0
reflcn data		
measured	5417	3953
unique	4998	3607
corrections	Lorentz−polarization	Lorenz−polarization empirical absorption (from 0.93 to 1.00 on *I*)
reflcn av	agreement on $I = 1.2\%$	agreement on $I = 1.1\%$
	C. Structure Solution and Refinement	
solution	Patterson method	Patterson method
refinement	full-matrix least-squares	full-matrix least-squares
minimization function	$\sum w(\|F_o\| - \|F_c\|)^2$	$\sum w(\|F_o\| - \|F_c\|)^2$
least-squares weights	$4F_o^2/\sum^2(F_o^2)$	$4F_o^2/\sum^2(F_o^2)$
anomalous dispersion	all non-hydrogen atoms	all non-hydrogen atoms
reflcns included	3361 with $F_o^2 > 3.0\sigma(F_o^2)$	3084 with $F_o^2 > 3.0\sigma(F_o^2)$
parameters refined	349	223
unweighted agreement factor	0.035	0.037
weighted agreement factor	0.045	0.055
esd of obd unit wt	1.49	2.16
convergence, largest shift	0.12σ	0.04σ
high peak in final diff map, e^{-1}/Å	0.21(4)	0.23(4)
Low peak in final diff map, e^{-1}/Å	−0.25(4)	−0.26(4)
computer hardware	VAX	VAX
computer software	SDP/VAX (Enraf-Nonius)[26]	MolEN (Enraf-Nonius)[27]

plexes from the paramagnetic four-coordinate[30] [TMP^{57}Fe] or [OEP^{57}Fe] was monitored in the same fashion. All proton chemical shifts for both porphyrinate and axial ligand resonances are in the diamagnetic region. The proton chemical shifts for coordinated PMe_3 in TMP and OEP complexes are also shielded by the ring current of the porphyrin, and appear at −2.36 and −3.08 ppm, respectively. In all bis(phosphine) complexes, the proton signal for coordinated trimethylphosphine is a triplet, as observed previously for other *trans*-bis(phosphine)metal complexes;[31] for our complexes, $J_{P-H} \approx 3$ Hz.

The mixed axial ligand compounds [Por$^{57}Fe^{II}(PMe_3)$(L)] were formed by stepwise titration of [Por$^{57}Fe^{II}$] with ligand L and PMe_3 and were monitored by ^{1}H NMR. As ligand L was added to [TPP$^{57}Fe^{II}$], the phenyl *o*-H resonance was observed to shift from 21.3 to ~8.1 ppm. During this process only one time-averaged *o*-H resonance was observed, thus indicating that intermediate spin (S = 1) [PorFe^{II}], high-spin (*S* = 2) [PorFe^{II}L], and low-spin (*S* = 0) [PorFe$^{II}L_2$] are in rapid chemical exchange on the ^{1}H NMR time scale. Once the bis(ligand) complex was formed, the titration of [Por$^{57}Fe^{II}(L)_2$] with PMe_3 was monitored by ^{31}P NMR. The titration was determined to be complete upon first detection of the ^{31}P NMR resonance associated to the bis(phosphine) complex [Por$^{57}Fe^{II}(PMe_3)_2$]. The ^{31}P resonances of [Por$^{57}Fe^{II}(PMe_3)$(L)] and [Por$^{57}Fe^{II}(PMe_3)_2$] appear as distinct peaks, indicating slow exchange of PMe_3 on the ^{31}P NMR time scale (Figure 1). However, any excess PMe_3 over the exact amount necessary to stoichiometrically form the mixed-ligand complex led to slow conversion to the $(PMe_3)_2$ complex.

(30) Balch, A. L.; Chan, Y.; Cheng, R.; La Mar, G. N.; Latos-Grazynski, L.; Renner, M. W. *J. Am. Chem. Soc.* **1984**, *106*, 7779.

(31) Bancroft, G. M.; Libbey, E. T. *Can. J. Chem.* **1973**, *51*, 1482. Dixon, K. R. Phosphorous to Bismuth. In *Multinuclear NMR*; Mason, J., Ed.; Plenum: New York, 1987; Chapter 13, pp 395−396.

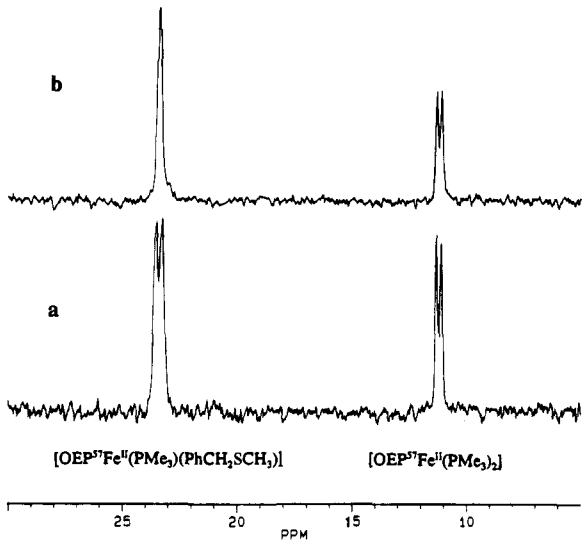

Figure 1. ^{31}P spectra of a solution containing a mixture of 94.5% ^{57}Fe-enriched $[OEP^{57}Fe^{II}(PMe_3)(PhCH_2SCH_3)]$ and $[OEP^{57}Fe^{II}(PMe_3)_2]$ at 21 °C in C_6H_6 (25 mM), recorded on a Bruker AM-500 spectrometer in the presence of broad band proton decoupling: (a) no ^{57}Fe decoupling; (b) on-resonance ^{57}Fe irradiation resulting in the decoupling of the $^{31}P-^{57}Fe$ doublet of $[OEP^{57}Fe^{II}(PMe_3)(PhCH_2SCH_3)]$. The chemical shift, relative to $Fe(CO)_5$, calculated from this on-resonance ^{57}Fe irradiation is $\delta_{Fe} = 9064$ ppm. Note that the doublet of $[OEP^{57}Fe^{II}(PMe_3)_2]$ ($\delta_{Fe} = 7873$ ppm) is unaffected by irradiation at the ^{57}Fe frequency of $[OEP^{57}Fe^{II}(PMe_3)(PhCH_2SCH_3)]$.

Synthesis of TMP and OEP mixed ligand complexes is described in the Experimental Section. Attempts to synthesize the mixed axial ligand compounds in the reverse addition order, by adding ligand L to $[Por^{57}Fe^{II}(PMe_3)_2]$, even in large excess, proved to be unsuccessful; clearly, the bis(phosphine) complex is the thermodynamic product of this titration. The proton signal of coordinated PMe_3 in mixed ligand complexes appears as a doublet, with $J_{P-H} \approx 8$ Hz.

Problems were encountered due to incomplete reduction of Fe(III) to Fe(II) (or re-oxidation, caused by impurities in some samples of solvent used). These problems were manifested by variations in the ^{31}P chemical shift of the bound trimethylphosphine as a function of reduction method (Zn(Hg) vs $NaBH_4$) or method of purification of the solvent. For example, preparations of $[TPPFe(PMe_3)_2]$ in d_6-benzene using Zn(Hg) as reductant typically resulted in a ^{31}P chemical shift of the coordinated PMe_3 of ~11.4 ppm, while preparation of $TPPFe^{II}$ in THF using $NaBH_4$ as reductant, followed by dissolution of the solid 4-coordinate $TPPFe^{II}$ in d_6-benzene and addition of PMe_3, yielded a ^{31}P chemical shift of 8.90 ppm. Since the Fe(III) complex, $[TPPFe(PMe_3)_2]^+$, has a ^{31}P chemical shift of ~36 ppm, the largest shift to higher shielding is taken as an indication of the purest Fe(II) preparation of the bis(phosphine) complex. It was routinely found that use of Zn(Hg) resulted in incomplete reduction, and we note that Sodano and Simonneaux, who used this reductant, also observed ^{31}P chemical shifts larger than those we have observed when $NaBH_4$ was used as reductant (13.5 ppm for $[TPPFe(PMe_3)_2]$ at 25 °C and 25.5 ppm for $[TPPFe(PMe_3)(N\text{-MeIm})]$ at −40 °C[25]). Interestingly, though the ^{31}P chemical shift of the coordinated trimethylphosphine was observed to vary by as much as 6 ppm, depending on preparation, the ^{57}Fe decoupling frequency never varied by more than 160 Hz, or no more than a 10 ppm change in the ^{57}Fe chemical shift. Thus, it is evident that while chemical exchange between the Fe(III) impurity and the desired Fe(II) form of $[TPPFe(PMe_3)_2]$ is rapid on the ^{31}P NMR time scale, it is slow on the ^{57}Fe NMR time scale. The 27 ppm difference in chemical shift of the ^{31}P resonance for the two oxidation states corresponds to a frequency difference $|\nu_{III} - \nu_{II}| \sim 5.5 \times 10^3$ Hz for the ^{31}P nucleus for the two chemically exchanging species, while the ^{57}Fe nucleus, where the unpaired electron of low-spin Fe(III) resides, at least to some extent in the 4s orbital (which has non-zero electron probability at the ^{57}Fe nucleus), is expected to have extremely large chemical shifts: Hyperfine couplings to ^{57}Fe in high-spin Fe(III) porphyrinates have been measured by ENDOR techniques ($A \sim 26-28$ MHz[32]), while for low-spin Fe(III) porphyrinates there have been reports for only a few complexes, in these cases measured by magnetic Mössbauer spectroscopic techniques ($A_{iso} \sim 61.3$ MHz for $[TPPFe(2\text{-MeImH})_2]^+$;[23] $A_{iso} \sim 58-70$ MHz for $[TMPFe(4\text{-}NMe_2Py)_2]^+$ [33]). Using the equation for the hyperfine contribution to the isotropic shift of paramagnetic complexes,[3]

$$\delta_{con} = A_{iso}hg\beta S(S+1)/3g_N\beta_N kT \qquad (1)$$

where A is in units of MHz and all other symbols have their usual meanings, we expect that at room temperature $|\nu_{III} - \nu_{II}| \sim 7.8-9.8 \times 10^5$ Hz, more than two orders of magnitude larger than for the ^{31}P nucleus. Thus, it is not surprising that the ^{57}Fe signals are in slow exchange while those of ^{31}P are in fast exchange. In fact, for typical solution concentrations of iron porphyrinate of 6−10 mM, this frequency separation would predict that if the ^{57}Fe chemical shift of the Fe(II) complex is unaffected by the presence of small amounts of the Fe(III) complex, then $k_{ex} \leq 6-7 \times 10^7$ M^{-1} s^{-1} for solutions of $[PorFeL_2]$ containing a fractional amount of the Fe^{III} complex. This value is within the range of measured exchange rate constants for model hemes of $1-17 \times 10^7$ M^{-1} s^{-1}.[34] Because of the variability of the ^{31}P chemical shift from preparation to preparation due to fast exchange between differing ratios of $[PorFe^{II/III}(PMe_3)_2]^{0/+}$, it may be somewhat surprising that a rough correlation was previously observed between the ^{31}P and ^{57}Fe chemical shifts.[17] However, in this study the samples were always *mainly* in the Fe(II) form, so the ^{31}P chemical shift still provided guidance as to the likely range of decoupling ^{57}Fe frequencies to be searched, as is discussed further below.

B. ^{57}Fe and ^{31}P Chemical Shifts. In Figure 1 is shown the ^{31}P spectra observed for two ^{57}Fe complexes present in the same NMR sample tube, $[OEP^{57}Fe^{II}(PMe_3)(PhCH_2SCH_3)]$ and $[OEP^{57}Fe^{II}(PMe_3)_2]$. The two complexes have different ^{57}Fe resonant frequencies, as is evidenced by the fact that one doublet, but not the other, is decoupled at a particular ^{57}Fe frequency. Stepping through the ^{57}Fe frequency range near 16.2 MHz in 100 Hz increments might be expected to be exceedingly time-consuming. However, as reported previously,[17] a rough correlation exists between the ^{31}P and the ^{57}Fe chemical shifts which makes it extremely simple to predict the ^{57}Fe shift of a new complex, thus easing the search for the proper ^{57}Fe decoupling frequency. This approximate correlation is borne out with the larger number of complexes that have now been investigated, as shown in Figure 2 and discussed below. Our 5 mm $\{^{57}Fe,^1H\}^{31}P$ probe provides excellent signal-to-noise ratio, which allows ^1H-decoupled ^{31}P spectra to be acquired on ~10 mM samples of $[Por^{57}Fe(PMe_3)_2]$ with 32−128 acquisi-

(32) Scholes, C. P. In *Multiple Electron Resonance Spectroscopy*; Dorio, M. M., Freed, J. H., Eds.; Plenum: New York, 1979; Chapter 8, pp 297−329.

(33) Safo, M. K.; Gupta, G. P.; Walker, F. A.; Scheidt, W. R. *J. Am. Chem. Soc.* **1991**, *113*, 5497.

(34) (a) Dixon, D. W.; Barbush, M.; Shirazi, A. *J. Am. Chem. Soc.* **1984**, *106*, 4638. (b) Shirazi, A.; Barbush, M.; Ghosh, S.; Dixon, D. W. *Inorg. Chem.* **1985**, *24*, 1081. (c) Dixon, D. W.; Woehler, S.; Hong, Z.; Stolzenberg, A. M. *Inorg. Chem.* **1988**, *27*, 3682. (d) Nesset, M. J. M. Ph.D. Thesis, University of Arizona, 1994.

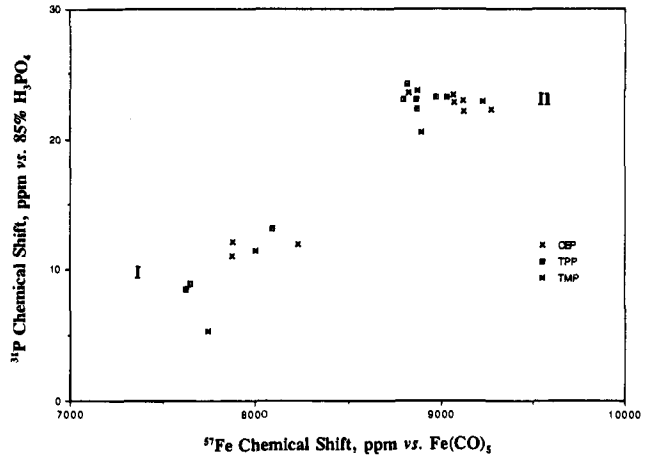

Figure 2. Correlation between ^{31}P and ^{57}Fe chemical shifts at 21 °C in C_6D_6, with ^{57}Fe shifts relative to external $Fe(CO)_5$ and ^{31}P shifts relative to external 85% H_3PO_4. All compounds and their respective chemical shifts are presented in Table 2.

tions. The ^{57}Fe−^{31}P coupling constants observed in this system (Table 2) are considerably larger than those found for iron coupled to nitrogen or carbon (J_{Fe-N} = ~8 Hz[14] or J_{Fe-C} = ~27 Hz[5]), thus permitting easier detection of the collapse of the observed phosphorus doublet than was possible in similar ^{15}N or ^{13}C labeled studies.

Figure 2 shows that rather than a smooth correlation between ^{31}P and ^{57}Fe chemical shifts, two general clusters are observed, cluster I, those in which the ^{31}P chemical shift ranges from 5 to 13 ppm while the ^{57}Fe chemical shift ranges from 7600 to 8200 ppm, and cluster II, those in which the ^{31}P chemical shift ranges from 22 to 24 ppm while the ^{57}Fe chemical shift ranges from 8800 to 9300 ppm. It should also be noted that cluster I includes only complexes that have PMe_3 opposite a relatively weak σ donor, relatively strong π acceptor ligand (PMe_3, CO, n-BuNC), while cluster II includes complexes that have PMe_3 opposite a relatively strong σ donor, which may or may not have π donor characteristics as well. As will be discussed further below, it is likely that the bonding interactions in these two types of complexes, types I and II, create quite different valence electron distributions about the metal, hence leading to quite different δ_{Fe} values.

The ^{57}Fe chemical shifts of the complexes investigated in this study are summarized in Table 2. It can be seen that replacement of electron withdrawing groups, −Cl (Hammett σ_p = +0.227[35]), by electron donating groups, $-OCH_3$ (Hammett σ_p = −0.268[35]), at the para positions of the phenyl rings of TPP causes a shift of the ^{57}Fe resonance to lower shielding (larger chemical shift). Chemical shifts of metal nuclei are generally interpreted in terms of screening constants, σ:

$$\sigma = \sigma^{dia} + \sigma^{para} \quad (2)$$

(Screening constants are, by convention, opposite in sign to chemical shifts and are defined with respect to the bare nucleus, while chemical shifts are defined with respect to a particular reference compound, in our case $Fe(CO)_5$.) Previous workers have concluded that the major factor that determines the chemical shifts of heavy nuclei (such as ^{57}Fe and ^{59}Co) is the paramagnetic term, σ^{para},[8c,36,37] which arises from the Ramsey formula:

$$\sigma^{para} = -(\mu_0 e^2/8\pi m^2)\sum_n (1/\Delta E_{0,n})[\langle 0|\sum_j r_j^{-3} l_{j\alpha}|n\rangle\langle n|\sum_j l_{j\beta}|0\rangle + \langle 0|\sum_j l_{j\beta}|n\rangle\langle n|\sum_j r_j^{-3} l_{j\alpha}|0\rangle] \quad (3)$$

where the matrix elements result from the unquenched orbital angular momentum of the paired electrons in the compounds of open-shell heavy atoms. For complexes of octahedral symmetry, this equation usually has one leading term, arising from a particular $\Delta E_{o,n}$ which is much smaller than any others, and hence dominates eq 3. This ΔE has been shown to be equal to the ligand field energy splitting of the metal complex.[8c,36,37] This explanation is believed to be particularly appropriate for low-spin d^6 ^{57}Fe(II) and ^{59}Co(III) complexes which are diamagnetic but have unfilled d-shells.[8c,36,37] For six-coordinate porphyrinate complexes of symmetry close to D_{4h} or C_{4v}, this lowest-energy d−d band splits into two transitions that are of similar magnitude, $\Delta E(^1A_1 \rightarrow {}^1A_2)$, corresponding to the excitation $d_{xy} \rightarrow d_{x^2-y^2}$, and $\Delta E(^1A_1 \rightarrow {}^1E)$, corresponding to the $\pi(d_{xz},d_{yz}) \rightarrow \sigma(d_{z^2},d_{x^2-y^2})$ transition, shown in one-electron symbols in Figure 3. For such complexes, with symmetry close to D_{4h} or C_{4v}, eq 3 reduces to[37c]

$$\sigma^{para} = -(8\mu_0\mu_B 2/\pi)\langle r_d^{-3}\rangle_F \left\{(1/3)\frac{\eta_{\sigma\pi}(^1A_2)}{\Delta E(^1A_2)} + (2/3)\frac{\eta_{\sigma\pi}(^1E)}{\Delta E(^1E)}\right\} \quad (4)$$

where $\langle r_d^{-3}\rangle_F$ is the average value of r^{-3} for the d-orbitals of the free ion, the $\eta_{\sigma\pi}$ are the reduction factors that arise from electron delocalization from metal to ligand due to σ or π covalency, and $\Delta E(^1A_2)$ and $\Delta E(^1E)$ are the two similar-energy electronic transitions shown in Figure 3. For a closely related set of axial ligands, both the screening constant and the chemical shift are expected to be inversely proportional to the two similar-magnitude ΔE values. It has been proposed that electron-releasing substituents on the porphyrinate ligand transmit electron density to the metal-based π orbitals (d_{xz}, d_{yz}) *via* the filled e(π) orbitals, thereby resulting in a decrease in ΔE and a concomitant increase in the magnitude of the σ^{para} term.[38] The results of this study that relate to para-substituted tetraphenylporphyrinates are consistent with this interpretation. However, it should also be noted that octaethylporphyrinate complexes consistently have larger ^{57}Fe chemical shifts (to lower shielding) than do their respective tetraphenylporphyrinate or tetramesitylporphyrinate analogs (Table 2). By the above argument, this would suggest that OEP is a stronger π donor ligand, while other spectroscopic and magnetic techniques have suggested instead that OEP is a stronger σ donor ligand than TPP. However, it is also possible that the π orbital mixing coefficients of TPP and OEP with the metal are different (due to different orbital energies), hence leading to changes in the sizes of the $\eta_{\sigma\pi}$ orbital reduction factors in eq (4). In support of this, the difference in ^{57}Fe chemical shift for the majority of the TPP and OEP complexes is a fairly constant 200−250 ppm, leading to the excellent correlation shown in Figure 4, while the differences in ^{57}Fe chemical shifts between TPP and TMP complexes vary randomly from −93 to +90 ppm, suggesting only minor differences in the bonding interactions in these two

(35) (a) Hammett, L. P. *Trans. Faraday Soc.* **1938**, *34*, 156. (b) Swain, C. G.; Lupton, E. C. *J. Am. Chem. Soc.* **1968**, *90*, 4328.

(36) Laszlo, P. In *NMR of Newly Accessible Nuclei*; Laszlo, P., Ed.; Academic Press: New York 1983; Vol. 2, pp 259−266.

(37) (a) Griffith, J. S.; Orgel, L. E. *Trans. Faraday Soc.* **1957**, *53*, 601. (b) Juranic, N.; Celap, M. B.; Vucelic, D.; Malinar, M. J.; Radivojsa, P. N. *J. Magn. Reson.* **1979**, *35*, 319. (c) Juranic, N. *Coord. Chem. Rev.* **1989**, *96*, 253.

(38) Bang, H.; Cassidei, L.; Danford, H.; Edwards, J. O.; Hagen, K. I.; Krueger, C.; Lachowitz, J.; Schwab, C. M.; Sweigart, D. A.; Zhang, Z. *Magn. Reson. Chem.* **1989**, *27*, 1117.

Table 2. ^{57}Fe and ^{31}P Chemical Shifts and Coupling Constants of ^{57}Fe(II) Porphyrinates Bound to Trimethylphosphine (PMe_3), T = 21 °C[a]

complex	δ_{Fe}, ppm	T dep (ppm/°C)	δ_P, ppm	T dep (ppm/°C)	J_{Fe-P} (Hz)
		Solvent = C_6D_6			
[(*p*-Cl)$_4$TPPFe(PMe$_3$)$_2$]	7623	+2.11	8.25	−0.028	41
[TPPFe(PMe$_3$)$_2$]	7652	+2.14	8.85	−0.027	45
[(*p*-OCH$_3$)$_4$TPPFe(PMe$_3$)$_2$]	7670	+2.34	9.91	-0.026	41
[TPPFe(PMe$_3$)(CO)]	7627		8.48		36
[TPPFe(PMe$_3$)(*n*-BuNC)]	8091		13.13		43
[TPPFe(PMe$_3$)(*n*-BuNH$_2$)]	8797		23.13		53
[TPPFe(PMe$_3$)(PhCH$_2$SCH$_3$)]	8813		24.23		56
[TPPFe(PMe$_3$)(NMeIm)]	8864		23.10		59
[TPPFe(PMe$_3$)(4-NMe$_2$Py)]	8883		19.75		52
[TPPFe(PMe$_3$)(Py)]	8973		23.29		59
[TPPFe(PMe$_3$)(4-CNPy)]	9033		23.24		53
[TMPFe(PMe$_3$)$_2$]	7743		5.32		43
[TMPFe(PMe$_3$)(*n*-BuNC)]	8001		11.46		42
[TMPFe(PMe$_3$)(PhCH$_2$SCH$_3$)]	8837		23.93		56
[TMPFe(PMe$_3$)(NMeIm)]	8827		23.58		53
[TMPFe(PMe$_3$)(4-NMe$_2$Py)]	8871		20.52		51
[TMPFe(PMe$_3$)(Py)]	8896		23.76		53
[OEPFe(PMe$_3$)$_2$]	7873		11.0		45
[OEPFe(PMe$_3$)(CO)]	7877		12.16		44
[OEPFe(PMe$_3$)(*n*-BuNC)]	8231		11.93		41
[OEPFe(PMe$_3$)(PhCH$_2$SCH$_3$)]	9064		23.43		47
[OEPFe(PMe$_3$)(NMeIm)]	9075		22.84		44
[OEPFe(PMe$_3$)(*n*-BuNH$_2$)]	9120		23.0		50
[OEPFe(PMe$_3$)(4-NMe$_2$Py)]	9128		22.20		53
[OEPFe(PMe$_3$)(Py)]	9224		22.91		50
[OEPFe(PMe$_3$)(4-CNPy)]	9275		22.36		49
		Solvent = d_8-Toluene			
[(*p*-OCH$_3$)$_4$TPPFe(PMe$_3$)$_2$]	7676		11.65		42
[(*p*-OCH$_3$)$_4$TPPFe(PMe$_3$)(NMeIm)]	8890		23.75		53
[TMPFe(PMe$_3$)$_2$]	7741		5.29		43
[TMPFe(PMe$_3$)(NMeIm)]	8824		23.95		53
[TMPFe(PMe$_3$)(2-MeImH)]	8893	+2.14	23.94	−0.027	52

[a] Abbreviations: *n*-BuNC = *n*-butylisocyanide, *n*-BuNH$_2$ = *n*-butylamine, PhCH$_2$SCH$_3$ = benzyl methyl sulfide, *N*-MeIm = *N*-methylimidazole, 2-MeImH = 2-methylimidazole, 4-NMe$_2$Py = 4-(dimethylamino)pyridine, Py = pyridine, 4-CNPy = 4-cyanopyridine.

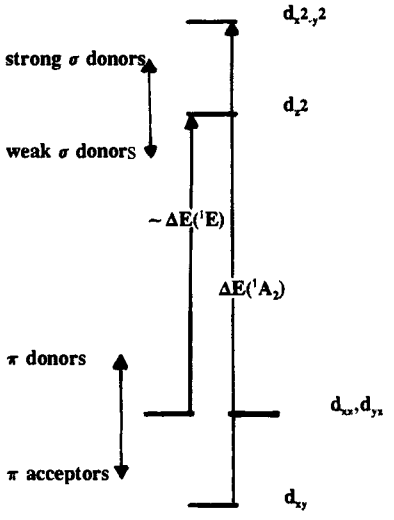

Figure 3. One-electron d-orbital energy level diagram for the d^6 Fe(II) porphyrinates of this study. The two lowest-energy d−d transitions, which are the major contributors to the paramagnetic screening constant, σ^{para}, are marked as $\sim\Delta E(^1E)$ and $\Delta E(^1A_2)$. The double-ended arrows show the expected effects of σ donor and π donor/acceptor interactions of axial ligands.

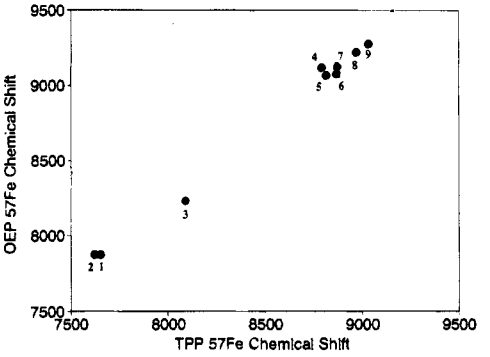

Figure 4. Correlation between ^{57}Fe chemical shifts of TPP and OEP complexes. Ligand combinations the following: 1, 2PMe$_3$; 2, PMe$_3$,-CO; 3, PMe$_3$,*n*-BuNC; 4, PMe$_3$,*n*-BuNH$_2$; 5, PMe$_3$,PhCH$_2$SCH$_3$; 6, PMe$_3$,NMeIm; 7, PMe$_3$,4-NMe$_2$Py; 8, PMe$_3$,Py; 9, PMe$_3$,4-CNPy.

porphyrinate ligands. Thus, there is no evidence of a major role for "steric hindrance" due to the *o*-CH$_3$ groups of the tetramesityl rings of [TMPFe(PMe$_3$)(L)] in determining the ^{57}Fe chemical shifts. This finding is consistent with the reports that for the related bis(pyridine) complexes of TMPFe^{III}, the mesityl groups do not hinder the rotation of axial ligands any more than do the phenyl rings of TPPFe^{III}, and in fact the barrier to rotation is even smaller in the TMP case,[39] nor do they hinder the binding of axial ligands to (2,6-Cl$_2$)$_4$TPPFe^{III} [40,41] or -Fe^{II},[41] or TMPFe^{III} or -Fe^{II}.[41]

The axial ligands are believed to transmit electron density to the metal by means of the ligand σ framework into the metal σ based orbital, d_{z^2},[18,19,42] which should cause an increase in $\Delta E(^1A_2)$ as the σ donor strength of the axial ligand increases. This leads to a ^{57}Fe shift to higher shielding (smaller chemical

(39) Safo, M. K.; Walker, F. A.; Raitsimring, A. M.; Walters, W. P.; Dolata, D. P.; Debrunner, P. G.; Scheidt, W. R. *J. Am. Chem. Soc.* **1994**, *116*, 7760.
(40) Hatano, K.; Safo, M. K.; Walker, F. A.; Scheidt, W. R. *Inorg. Chem.* **1991**, *30*, 1643.
(41) Nesset, M. J. M.; Shokhirev, N. V.; Jacobson, S. E.; Walker, F. A. Manuscript in preparation.
(42) Hagen, K. I.; Schwab, C. M.; Edwards, J. O.; Sweigart, D. A. *Inorg. Chem.* **1986**, *25*, 978.

shift) for [TPP^{57}Fe^{II}(PMe$_3$)(L)] and [OEP^{57}Fe^{II}(PMe$_3$)(L)] where L is a series of closely-related ligands, such as 4-(dimethylamino)pyridine as compared to pyridine and 4-cyanopyridine. This same trend was previously observed for the related series of compounds [(protoporphyrin-IX)Fe(CO)(L)], where L = a series of pyridines of varying σ donor strengths.[18] Other similarities found between the two studies are that we observe the chemical shift of [TPP^{57}Fe^{II}(PMe$_3$)(NMeIm)] to be distinctly smaller than those of the pyridine complexes, suggesting that if only σ bonding effects are important, *N*-MeIm is a stronger σ donor than any of the pyridines. Also, when *N*-methlyimidazole is replaced by the more sterically hindered 2-methylimidazole in [TMP^{57}Fe^{II}(PMe$_3$)(L)], only a small increase in the ^{57}Fe chemical shift is observed.

The combination of effects of both TPP and axial ligand substituents on ^{57}Fe chemical shifts suggests the 1-electron d-orbital energy level diagram shown in Figure 3, where $\Delta E(d_{xz},d_{yz}\rightarrow d_{z^2})$ is approximately equal to $\Delta E(^1E)$ and is the lowest-energy d−d transition. $\Delta E(d_{xy}\rightarrow d_{x^2-y^2})$ or $\Delta E(^1A_2)$ is of similar energy. The major expected effects of axial σ donation and π donor−acceptor interactions of both axial ligands and porphyrinate on the size of $\Delta E(^1E)$ are indicated by the arrows. At the point where exceptionally strong π acceptor behavior or exceptionally strong σ donor behavior changes the ordering of the orbital energies, the relative magnitudes of $\Delta E(^1E)$ and $\Delta E(^1A_2)$ will reverse, but they will probably never differ by more than 20−30%. It should be noted that covalency will mix the d_{xz},d_{yz} metal orbitals with the e(π) symmetry porphyrin and π or π^* axial ligand orbitals, and σ symmetry axial ligand orbitals with the d_{z^2} orbital, in each case leading to changes in $\eta_{\sigma\pi}$ (eq 4), but that the d_{xy} orbital cannot mix with any porphyrin π orbital without significant ruffling of the porphyrinate ring.[39] Hence, orbital reduction factors $\eta_{\sigma\pi}$ of eq 4 may vary in magnitude as the type of axial ligand (or porphyrinate substituent) changes significantly, and thus modulate the effect of changes in $\Delta E(^1E)$ and $\Delta E(^1A_2)$.

Most model hemes and heme proteins investigated thus far, except for cytochrome *c*, have ^{57}Fe chemical shift values ranging from 7200 to 9200 ppm. However, most of them also have at least one π acceptor ligand (CO, RNC, or PMe$_3$). In contrast to these systems, the ^{57}Fe resonance of cytochrome *c* is dramatically shifted to lower shielding (11 197 ppm).[9] However, cytochrome *c* is the only one in which both the axial ligands are *both* strong σ donors and strong π donors. Only one report was available when we began this work of the direct detection of the ^{57}Fe resonances of bis(amine) complexes of TPP^{57}Fe^{II}, that of the bis(d_5-pyridine) and bis(pyrrolidine) complexes.[14] The ^{57}Fe chemical shifts were reported to be 7341 and 7258 ppm, respectively, lower values than those of all reported [PFeL(CO)] complexes, and in fact, lower than for all other Fe(II) porphyrinates reported to date. In view of the trends in chemical shifts observed for mixed-ligand PMe$_3$-(substituted pyridine) complexes (Table 2, Figures 2 and 4), as well as the Mössbauer spectra of a variety of Fe(II) porphyrinates, discussed elsewhere,[43] we have reinvestigated the bis(pyridine) complex, [TPPFe(Py)$_2$], by direct detection methods, and found the true chemical shift to be 11,723 ppm, with a temperature dependence of +2.9 ppm/deg.[43] Both the chemical shift and temperature dependence of this ^{57}Fe signal are similar to those of ferrocytochrome *c*.[9] The Mössbauer−NMR correlation used to aid in finding this signal[43] suggests that it is likely that most other bis(amine), bis(thioether), or amine−thioether mixed-ligand complexes of iron(II) porphyrinates will be found to have ^{57}Fe chemical shifts in the 10000−14000 ppm range, and that these complexes also follow the ligand field and covalency predictions of eq 4.

(43) Polam, J. R.; Wright, J. L.; Christensen, K. A.; Walker, F. A.; Flint, H.; Winkler, H.; Grodzieki, M.; Trautwein, A. X. *J. Am. Chem. Soc.* Submitted for publication.

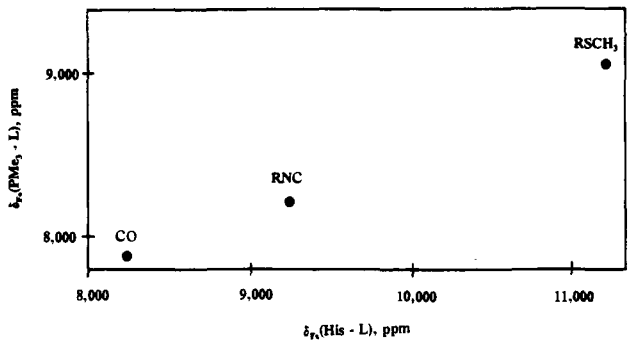

Figure 5. Chemical shift correlation between OEP^{57}Fe^{II} complexes having PMe$_3$−L axial ligand combinations (Table 2) and heme proteins having histidine−L combinations. The heme proteins are myoglobin-CO,[5,21,22] myoglobin−butyl isocyanide,[13] and cytochrome *c*.[9]

As a qualitative example of the behavior of ^{57}Fe(II) porphyrinates according to eq 4, it should be noted that each of the three series of porphyrinate complexes investigated, TPP, TMP, and OEP, showd a large increase in ^{57}Fe chemical shift for the series [Por^{57}Fe^{II}(PMe$_3$)(L)], where L = CO, butyl isocyanide, and PhCH$_2$SCH$_3$ (Table 2). This may be compared to the ^{57}Fe chemical shift trend observed for carbonmonoxymyoglobin,[5,21,22] butyl isocyanide myoglobin,[13] and ferrocytochrome *c*,[9] where histidine is the second axial ligand in each case. The correlation of these chemical shifts for model hemes and heme proteins shown in Figure 5 suggests that the effect of a given ligand is similar in both cases but is amplified when placed opposite a strong σ-donating ligand as compared to a weak σ-donor, strong π acceptor.

Benn and co-workers have investigated the use of 2-D indirect detection of ^{57}Fe chemical shifts for organoiron complexes[10a-c] and found that substituents at phosphorus affect the σ-donor/π-acceptor ability of the phosphorus ligand, and strong π-acceptor phosphine ligands lead to an enhanced shielding of the iron nucleus. The authors concluded that the $1/\Delta E$ dependence of $\delta(^{57}Fe)$ reflects the donor/acceptor ability of the phosphorus ligand.[10] This $1/\Delta E$ dependence was found to correlate with the reduction potentials of the same series of complexes measured by cyclic voltametric techniques, and a similar correlation is observed between ^{57}Fe chemical shifts, the paramagnetic shielding term $1/\Delta E$, and the reduction potentials of a variety of ferrocenes.[10d]

It has been suggested that the chemical shift anisotropy term, $\Delta\delta = |\delta_{||} - \delta_{\perp}|$, is important in determining the line widths of ^{57}Fe signals, and that the average chemical shift, $\delta = (1/3)\delta_{||} + (2/3)\delta_{\perp}$, should be used instead of the paramagnetic screening term, σ_{para}, to predict ^{57}Fe NMR shifts.[9,21] The magnetic shielding constant σ can be defined for axially symmetric molecules in terms of $\sigma_{||}$, the parallel screening constant tensor element along the major molecular axis, and $\sigma_{\perp}$, the tensor element perpendicular to it. It has been proposed by Baltzer that the value of $\sigma_{\perp}$ for all porphyrinate systems is roughly the same, corresponding to a chemical shift element $\delta_{\perp}$ of about -9000 ppm.[9] Thus, according to Baltzer, it is the screening constant element $\sigma_{||}$ which differentiates the chemical shift values of individual ^{57}Fe-substituted model hemes and heme proteins.[9] Based upon this premise, and adding to it the hypothesis that one PMe$_3$ ligand, common to all of our complexes, should provide a fairly constant contribution to $\sigma_{||}$,[9] it might be possible to predict the ^{57}Fe chemical shifts by using the differential chemical shift contribution for the bis(trimethylphosphine)

complex and the desired mixed-ligand complex:

$$\delta_{(L)(L')} = \delta_{(L)(PMe_3)} + \delta_{(L')(PMe_3)} - \delta_{(2PMe_3)} \quad (5)$$

The results of such predictions are mixed. For the *n*-butyl isocyanide−*N*-methylimidazole combination we predict a chemical shift of 9405 ppm for the TPP complex and 9433 ppm for the OEP complex, both of which compare reasonably well to the chemical shift of the *n*-butyl isocyanide complex of myoglobin (9238 ppm).[13] The same method predicts that all bis(amine) and bis(thioether) complexes should have ^{57}Fe chemical shifts of 9900−10700 ppm, and it should be noted that the chemical shifts of ferrocytochrome *c* and [TPPFe(d_5-Py)$_2$] are just on the outside edge of this range, at 11 197[9] and 11 723 ppm,[43] respectively. However, the predicted chemical shifts of all [PorFe(CO)(L)] complexes are ~700−1100 ppm larger than those observed.[5,12,18,19,21] In fact, it is already evident when one considers the similarity in chemical shift of the bis(trimethylphosphine) (7623−7873 ppm, Table 2) and the mixed-ligand (CO)−(trimethylphosphine) complexes (7627−7877 ppm, Table 2), as compared to the large difference in chemical shifts of the [PorFe(CO)(L)] (~8000−8200 ppm)[5,12,18,19,21] and [PorFe(PMe$_3$)(L)] complexes (8797−9275 ppm, Table 2), that this approach does not work well when a very strong π acceptor ligand, such as CO, is present. Thus, it appears that ligand effects on metal shielding cannot be assumed to be additive in the presence of substantial electronic interaction (delocalization) from metal to ligand and vice versa, and eq 5 provides only a crude prediction of the chemical shifts of Fe(II) porphyrinates.

Finally, we are reminded of the conclusion of Sams[6] and Sato,[7] based on Mössbauer data, that the porphyrinate macrocycle has an "electron sink capability," that compensates for the electronic properties of axial ligands. Neither our ^{57}Fe and ^{31}P NMR data presented herein (which show clear differentiation between complexes in which both axial ligands are weak σ donors, strong π acceptors (type I) and those in which one axial ligand is of this type while the other is a strong σ donor, weak π acceptor (type II)), and those in which both axial ligands are strong σ donors and weak π acceptors (cytochrome c[9] and [TPPFe(d$_5$-Py)$_2$][43]), nor Mössbauer data for the same series of complexes (which show a strong increase in ΔE_Q when one and then a second weak σ donor, strong π acceptor ligand(s) are replaced by strong σ donor, weak π acceptor ligands[43]) are consistent with there being an "electron sink capability" of the porphyrinate macrocycle.

C. Comparison of d^6 ^{57}Fe and ^{59}Co Porphyrinates. Sweigart, Edwards, and co-workers have proposed that ^{57}Fe(II) chemical shifts may be predicted from the chemical shift values obtained for isoelectronic, isostructural ^{59}Co(III) complexes.[42,44] The advantage of using ^{59}Co chemical shifts to predict those of ^{57}Fe is that ^{59}Co is 100% naturally abundant and has detection sensitivity 4×10^5 times larger than that of iron at natural abundance, or almost 10^4 times larger than for our 94.5% enriched ^{57}Fe samples. However, there are also important differences between ^{57}Fe and ^{59}Co that detract from the use of the latter: (1) cobalt has a nuclear spin $I = 7/2$ and a relatively large quadrupole moment of 0.4×10^{-28} cm^2, which causes ^{59}Co line widths to be sensitive to electric field gradients at the nucleus, and thus to the symmetry about the cobalt atom;[45,46] and (2) Co(III) porphyrinates bound to neutral axial ligands have a formal positive charge, which results in ^{59}Co chemical shift values and line widths being strongly affected by counterions and solvent effects due to the positive charge on the complex.[47] This, we expected, would not be the case for the neutrally charged Fe(II) porphyrins. Indeed, we find much less solvent dependence for ^{57}Fe(II) porphyrinates than for the ^{59}Co(III) counterparts (see part E).

In comparing the ^{59}Co chemical shifts reported for [(*p*-X)$_4$TPP^{59}Co(HIm)$_2$]$^+$BF$_4^-$ (X = Cl, H, OCH$_3$, δ = 8446, 8447, 8459 ppm, respectively (with respect to Co(CN)$_6^{3-}$),[42] a range of 13 ppm) to the ^{57}Fe chemical shifts of [(*p*-X)$_4$TPP^{57}Fe(PMe$_3$)$_2$] (X = Cl, H, OCH$_3$, δ = 7621, 7650, 7664 ppm, respectively, a range of 43 ppm) the trend is in the same direction, but a linear correlation is not apparent. Hence, differences in solvation of the Co(III) complexes may be more important than substituent effects.

Line broadening of the ^{59}Co resonance of many cobalt(III) porphyrinates[38] limits the possibility of carrying out a comprehensive study of complexes having a variety of axial ligands, and especially mixed-ligand systems. The ^{59}Co chemical shift values reported for all the various bis(imidazole) complexes reported thus far fall within an 88 ppm window (8821 to 8733 ppm), whereas the line widths vary by more than an order of magnitude from 103 Hz to 2278 Hz.[38] For cobalt porphyrinates having two axially coordinated pyridine ligands, the line widths are reported to be in the range of 11 kHz,[38,48] and no ^{59}Co NMR signal could be detected for [TPPCo(PMe$_3$)$_2$]$^+$.[48]

D. Temperature Dependence of the ^{57}Fe and ^{31}P Chemical Shifts. We have investigated the temperature dependence of the ^{57}Fe and ^{31}P chemical shifts for [(*p*-Cl)$_4$TPPFe(PMe$_3$)$_2$], [TPPFe(PMe$_3$)$_2$], and [(*p*-OCH$_3$)$_4$TPPFe(PMe$_3$)$_2$] over the range of −61 to +30 °C in toluene-d_8 and from 20 to 55 °C in benzene-d_6 and for [TMPFe(PMe$_3$)(2-MeImH)] from −100 to +30 °C in toluene-d_8. Linear shifts of both ^{57}Fe and ^{31}P resonances with temperature were observed above −60 °C, with the ^{57}Fe and ^{31}P chemical shifts having opposite temperature dependences. Example data, for [TMPFe(PMe$_3$)(2-MeImH)], are shown in Figure S1, supporting information. The temperature dependences of the ^{57}Fe chemical shifts (+2.1−2.3 ppm/°C, Table 2) are similar to that found for ferrocyctochrome *c*[9] and to those found for ^{59}Co chemical shifts.[42,44] An increase in temperature is expected to result in a lower average energy of the $d_\pi \rightarrow d_\sigma$ transition $\Delta E(^1E)$ by increasing the occupancy of the higher vibrational levels of the ground electronic state,[46,49] hence increasing the ^{57}Fe chemical shift. For the ^{31}P signal the explanation of the opposite temperature dependence is not as obvious. However, both the 5-coordinate [TPPZnPMe$_3$] complex and PMe$_3$ itself also display smaller shifts of the ^{31}P signal to higher shielding with increasing temperature (−0.014 and −0.005 ppm/°C, respectively) (data not shown). Similar temperature dependence for ^{31}P has also previously been reported for organophosphate ester systems.[50] Neither ^{31}P nor ^{57}Fe chemical shifts were affected by changes in [TPPFe(PMe$_3$)$_2$] concentration from 6 to 24 mM.

E. Solvent Effects on the ^{57}Fe and ^{31}P Chemical Shifts. We have measured the ^{57}Fe and ^{31}P chemical shifts in five different solvents (benzene, toluene, tetrahydrofuran, dichloromethane, and chloroform). There is not much solvent dependence on either ^{57}Fe or ^{31}P chemical shifts, and the small

(44) Hagen, K.; Schwab, C. M.; Edwards, J. O.; Lawler, R. G.; Sweigart, D. A. *J. Am. Chem. Soc.* **1988**, *110*, 7024.
(45) Au-Yeung, S. C. F.; Eaton, D. R. *J. Magn. Reson.* **1983**, *52*, 351.
(46) Harris, B. K; Mann, B. E. *NMR and the Periodic Table*; Academic Press: London, 1978.
(47) Sotomayor, J.; Santos, H.; Pina, F. *Can. J. Chem.* **1991**, *69*, 567.
(48) Walker, F. A.; Hawkins, C. J. Unpublished results.
(49) Benedek, G. B.; Englman, R.; Armstrong, J. A. *J. Chem Phys.* **1963**, *39*, 3349.
(50) (a) Jameson, C. J.; Jameson, A. K.; Parker, H. *J. Chem. Phys.* **1978**, *68*, 2868. (b) Jameson, C. J.; de Dios, A. C.; Jameson, A. K. *J. Chem. Phys.* **1991**, *95*, 1069.

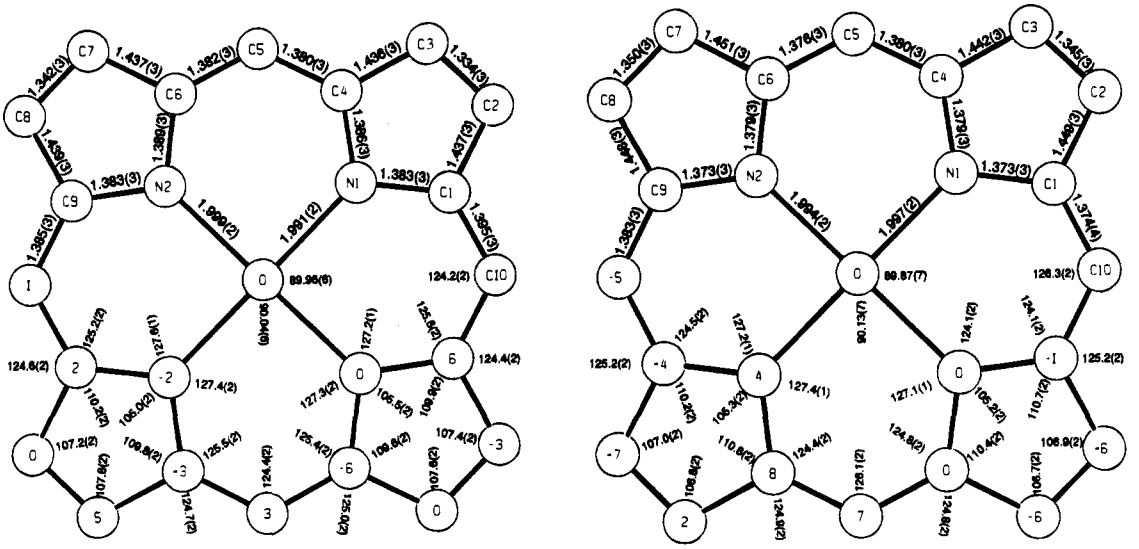

Figure 6. Formal diagram of the porphinato core of (a) $[(p\text{-}OCH_3)_4TPP^{57}Fe^{II}(PMe_3)_2]$ and (b) $[OEP^{57}Fe^{II}(PMe_3)_2]$. Displayed on the upper half of each are the bond lengths and the numbering scheme. On the lower half of each diagram the bond angles and the numbered symbols for each atom are replaced by its perpendicular displacement, in units of 0.01 Å, from the mean plane of the porphinato core.

differences that exist (a total difference of 16 ppm) do not appear to correlate with any common measure of solvent interaction (dielectric constant, Gutman's donor number,[51] or Reichardt's E_T[52]). For comparison of $[TMP^{57}Fe(PMe_3)_2]$ in three solvents of varying dielectric constant and donor number ($CHCl_3$, CH_2Cl_2, THF) to $[TPP^{59}Co(ImH)_2]BF_4$ in the same series of solvents, the ^{57}Fe chemical shifts differ by only 13 ppm, while the ^{59}Co chemical shifts in the same three solvents differ by 68 ppm.[42,53] Hence, it is clear that the ^{57}Fe chemical shifts do not depend on the solvent nature nearly as strongly as do ^{59}Co chemical shifts in d^6 metalloporphyrinates.

F. Structures of $[(p\text{-}OCH_3)_4TPP^{57}Fe^{II}(PMe_3)_2]$ and $[OEPFe^{II}(PMe_3)_2]$. The crystal and molecular structures of $[(p\text{-}OCH_3)_4TPPFe^{II}(PMe_3)_2]$ and $[OEPFe^{II}(PMe_3)_2]$ have been determined by X-ray crystallography. The formal diagrams of the porphyrinato cores of the two complexes are shown in Figure 6, parts a and b, respectively, and the ORTEP diagrams in Figure 7, parts a and b, respectively. All bond lengths, angles, and thermal parameters are of their expected values for a six-coordinate bis(phosphine) iron(II) porphyrinate.[25,54] The porphyrinato core of the TPP derivative is not rigorously planar, with the maximum deviation from the mean plane being 0.06 Å (Figure 6a). All bond distances and bond angles are given in Tables S1-S4. The Fe−P distances of known (porphyrinato)iron(II)−bis(phosphine) complexes are compared in Table 3. For $[(p\text{-}OCH_3)_4TPPFe(PMe_3)_2]$ (this work) the Fe−P distance is 2.2968(6) Å, similar to the reported values for $[TPPFe^{II}(PMe_2Ph)_2]$[25] and $[TPPFe^{II}(P(n\text{-}Bu)_3)_2]$[54] of 2.284 and 2.346 Å, respectively. The Fe−N_P bond distances of 1.991(2) and 1.999(2) Å are similar to those of the two closely related complexes.[25,54] As required for $\bar{1}$ symmetry, the axial bond angle P−Fe−P is undistorted (180.(0)°). There is a slight distortion away from 90° for the P−Fe−N angles; the largest deviation is 1.02°. The dihedral angles between the phenyl rings and the mean plane of the porphyrinate are 72.45(6)° and 71.57(7)°, similar to that found for $[TPPFe^{II}(PMe_2Ph)_2]$.[25]

There is no solvent molecule in the crystal structure of $[OEPFe^{II}(PMe_3)_2]$, but there are two molecules of benzene per

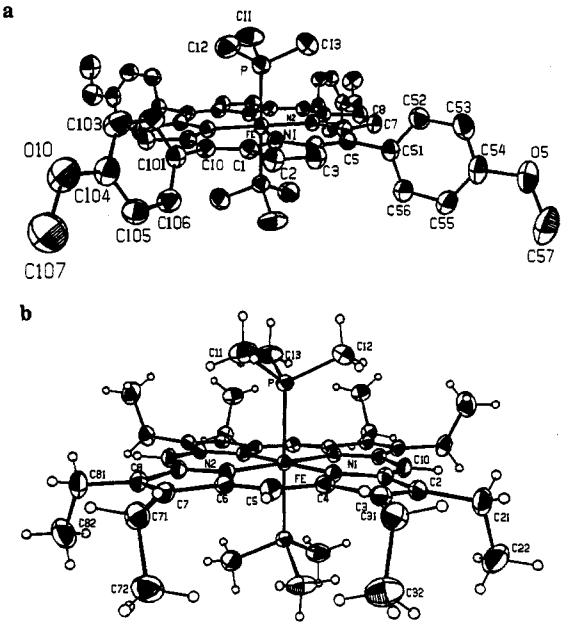

Figure 7. A perspective view of (a) $[(p\text{-}OCH_3)_4TPP^{57}Fe^{II}(PMe_3)_2]$ and (b) $[OEP^{57}Fe^{II}(PMe_3)_2]$ with atom numbering.

unit cell of $[(p\text{-}OCH_3)_4TPPFe^{II}(PMe_3)_2]$ (Figure 6). This is therefore another of nearly 100 "isostructural" triclinic porphyrin structures. These types of porphyrin-based lattice clathrates have been classified as "porphyrin sponges".[55] In porphyrin sponges the guest:host stoichiometry can vary from 1:1 to 5:1 ratio with the 2:1 stoichiometry being the most prevalent. In this context the $[(p\text{-}OCH_3)_4TPPFe^{II}(PMe_3)_2]$ is the host and two C_6D_6 solvent molecules are the guests. The benzene molecules are approximately parallel to each other, as shown in Figure S2, supporting information. These solvent molecules are contained in a column which passes through the unit cell in the *b*-direction. The sides of the column are defined by the phenyl substituents of surrounding porphyrin molecules. Each of these three molecules sits around a crystallographic inversion center. The Fe was defined to be at (0,0,0), Wyckoff position a. The

(51) Gutmann, V. *Chimia* **1977**, *31*, 1.
(52) Reichardt, C. *Angew. Chem., Int. Ed. Engl.* **1965**, *4*, 29.
(53) Bang, H.; Edwards, J. O.; Kim, J.; Lawler, R. G.; Reynolds, K.; Ryan, W. J.; Sweigart, D. A. *J. Am. Chem. Soc.* **1992**, *114*, 2843.
(54) Belani, R. M.; James, B. R.; Dolphin, D.; Rettig, S. T. *Can. J. Chem.* **1988**, *66*, 2072.
(55) (a) Byrn, M. P.; Curtis, C. J.; Khan, S. I.; Sawin, P. A.; Tsurumi, R.; Strouse, C. E. *J. Am. Chem. Soc.* **1990**, *112*, 1865. (b) Bryn, M. P.; Curtis, C. J.; Goldberg, I.; Hsiou, Y.; Khan, S. I.; Sawin, P. A.; Tendick, K.; Strouse, C. E. *J. Am. Chem. Soc.* **1991**, *113*, 6549.

Table 3. Bond Lengths and Degree of Planarity of the Porphyrinato Ring for a Series of Six-Coordinate Iron Porphyrinates

complex	Fe−P, Å	Fe−N_P, Å	max deviation from mean plane, Å	ref
$[OEPFe^{II}(PMe_3)_2]$	2.2750(6)	1.997(2) 1.994(2)	0.08	this work
$[(p\text{-}OCH_3)_4TPPFe^{II}(PMe_3)_2]$	2.2968(6)	1.991(2) 1.999(2)	0.06	this work
$[TPPFe^{II}(PBu_3)_2]$	2.346(1)	1.998(3)	planar	54
$[TPPFe^{II}(PMe_2Ph)_2]$	2.284(1)	2.000(1)	planar	25
$[TPPFe^{III}(PMe_2Ph)_2]^+$	2.350(1)	1.990(2)	planar	25

benzene molecules are centered at ($^1/_2$,0,$^1/_2$) and ($^1/_2$,$^1/_2$,$^1/_2$), Wyckoff positions f and h, respectively. Stereo unit cell packing diagrams were generated to help visualize the packing and look for potential molecular interactions. The diagrams show that neither the porphyrinato core, the phenyl substituents, nor the solvent benzene molecules are involved in any stacking interactions.

In contrast to $[(p\text{-}OCH_3)_4TPPFe(PMe_3)_2]\cdot 2C_6D_6$, $[OEPFe(PMe_3)_2]$ contains no solvent of crystallization. Again, the porphyrinate ring is essentially planar; deviations from planarity are given in Figure 6b. There is no π-stacking of the OEP rings in the crystal. Rather, the molecules are packed in a "herringbone" pattern along the *c*-axis. Each porphyrinate ring is tilted 65.7° with respect to the *c*-axis, and the interplanar separation is 9.23 Å.

Summary and Conclusions. An indirect 1-D NMR technique that utilizes the sensitive ^{31}P nucleus as the detected signal, together with the coordination of one or two phosphine ligands to the axial positions of Fe(II) model hemes, has allowed determination of the ^{57}Fe chemical shifts of new complexes by decoupling the $^{57}Fe-^{31}P$ doublet of enriched $^{57}Fe(II)$ porphyrins. A rough correlation has been found between ^{31}P and ^{57}Fe chemical shifts that makes it easy to predict the ^{57}Fe chemical shift of new complexes, thus simplifying the search for the proper decoupling frequency. ^{57}Fe chemical shifts of substituted phenyl TPPs and substituted axial pyridine ligands follow the predicted trends based on the paramagnetic screening constant, σ^{para}, for heavy nuclei being the dominant factor. The axial ligand CO in mixed-ligand $(PMe_3)(CO)$ combination produces a similar ^{57}Fe chemical shift to that of the $(PMe_3)_2$ complex (7627, 7652 ppm (TPP)), and the $(PhCH_2SCH_3)(PMe_3)$ combination produces a similar ^{57}Fe chemical shift to that of (*N*-MeIm)(PMe_3) (8813, 8864 ppm (TPP)). Two strong σ donor axial ligands produce the largest ^{57}Fe chemical shifts, in the 11000−12000 ppm range. ^{31}P and ^{57}Fe chemical shifts both show linear temperature dependence, but with opposite slopes.

Acknowledgment. The support of the National Institutes of Health (Grant No. DK 31038) and the University of Arizona Materials Characterization Program is gratefully acknowledged. The authors acknowledge helpful discussions with Professors John H. Enemark and Alfred X. Trautwein.

Supporting Information Available: Tables S-1 to S-4 of positional parameters, general displacement parameters, least-squares planes, dihedral angles between planes for $[(p\text{-}OCH_3)_4TPP^{57}Fe(PMe_3)_2]$ and $[OEP^{57}Fe(PMe_3)_2]$; Figure S-1, showing temperature dependence of the ^{57}Fe and ^{31}P chemical shifts of [TMPFe(PMe_3)(2−MeImH)], and Figure S-2, showing crystal packing of the "sponge porphyrin", $[(p\text{-}OCH_3)_4TPP^{57}Fe(PMe_3)_2]$ (7 pages). This material is contained in many libraries on microfiche, immediately follows this article in the microfilm version of the journal, and can be ordered from the ACS; and can be downloaded from the Internet; see any current masthead page for ordering information and Internet access instructions.

JA9509691